THE JOURNAL OF PHYSICAL CHEMISTRY B

ARTICLE

pubs.acs.org/JPCB

Exploring the Strength, Mode, Dynamics, and Kinetics of Binding Interaction of a Cationic Biological Photosensitizer with DNA: Implication on Dissociation of the Drug−DNA Complex via Detergent Sequestration

Bijan Kumar Paul and Nikhil Guchhait*

Department of Chemistry, University of Calcutta, 92 A. P. C. Road, Calcutta-700009, India

Supporting Information

ABSTRACT: The present study aims at exploring a detailed characterization of the binding interaction of a promising cancer cell photosensitizer, harmane (HM), with DNA extracted from herring sperm. The polarity-sensitive prototropic transformation of HM, a naturally occurring, fluorescent, drug-binding alkaloid, β-carboline, is remarkably modified upon interaction with DNA and is manifested through significant modulations on the absorption and emission profiles of HM. From the series of studies undertaken in the present program, for example, absorption; steady-state emission; the effect of chaotrope (urea); iodide ion-induced steady-state fluorescence quenching; circular dichroism (CD); and helix melting from absorption spectroscopy; the mode of binding of HM into the DNA helix has been substantiated to be principally intercalative. Concomitantly, a discernible dependence of the photophysics of the DNA-bound drug on the medium ionic strength indicates that electrostatic attraction should not be ignored in the interaction. Efforts have also been delivered to delineate the dynamical aspects of the interaction, such as modulation in time-resolved fluorescence decay and rotational relaxation dynamics of the drug within the DNA environment. In view of the prospective biological applications of HM, the issue of facile dissociation of intercalated HM from the DNA helix also comprises a crucial prerequisite for the functioning as an effective therapeutic agent. In this context, our results imply that the concept of detergent-sequestered dissociation of the drug from the drug−DNA complex can be a prospective strategy through an appropriate choice of the detergent molecule. The utility of the present work resides in exploring the potential applicability of the fluorescence property of HM for studying its interactions with a relevant biological target, for example, DNA. In addition, the methods and techniques used in the present work can also be exploited to study the interaction of HM with other biological, biomimicking assemblies and drug delivery vehicles, and so forth.

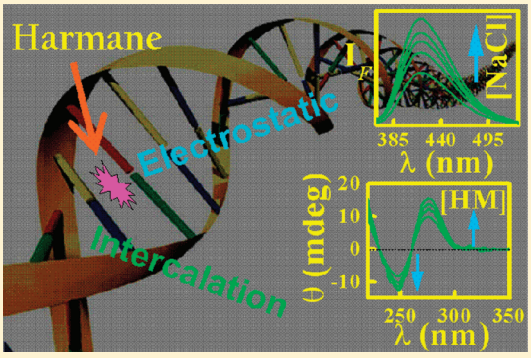

1. INTRODUCTION

Deoxyribonucleic acid (DNA) that contains the genetic instructions for the development and functioning of living organisms is an obvious focus of attraction for many researchers.[1−3] DNA can rightfully be described as one of nature's most elementary conduits for carrying the "blueprint" of instructions for the development of other essential components of living systems, such as proteins, cells, and RNA.[1−3] Therefore, quite unambiguously, it has formed the nucleus of many-faceted research activities for years. One such interesting subject of research surrounding DNA has been the recognition and characterization of the interaction of small molecules with DNA as they yield effective information for the development of therapeutic agents in controlling gene expression.[4−9] The study of the interaction of small molecules with DNA is of huge significance in view of their ability to function as a rational design system for the development of new efficient drugs targeted to DNA, to serve as sensitive molecular reporters for monitoring nucleic acid structure, and so forth.[10−12] However, the affinity, strength and mode of interaction of small molecules with biopolymers are governed by various structural and electronic factors.[4−20] In this study, we demonstrate a spectral deciphering of the interaction of harmane (HM), which belongs to the family of naturally occurring fluorescent drug-binding alkaloids β-carbolines, with DNA extracted from herring sperm.

The interest focused on the photophysical properties of the natural product, β-carbolines, has principally emanated from their widespread biological properties. These include their functions as potential monoamine oxidase enzyme inhibitors and their interaction with a considerable number of neurotransmitters and neuromodulators of the central nervous system.[21−23] In addition, the novel biological application of β-carbolines in the form of photosensitizers to fungi, viruses, bacteria, etc. has been central to an immensely important topic of research in medical

Received: July 12, 2011
Revised: September 2, 2011
Published: September 07, 2011

dx.doi.org/10.1021/jp206589e | J. Phys. Chem. B 2011, 115, 11938–11949

science, photodynamic therapy.[24,25] β-Carbolines are reported to be effective in producing singlet oxygen, which is detrimental to cancerous cells.[26,27] Naturally, the interaction of β-carboline derivatives with relevant biological receptors forms a prospective avenue for biophysical and biochemical research, which still awaits much investigation. In addition, the presently studied molecular system HM has remained comparatively underutilized in these studies and, hence, demands meticulous exploration.

The present work is focused on the binding interaction of the cationic biological photosensitizer HM with DNA. Steady-state absorption, emission, and circular dichroic spectroscopic techniques have been employed to delve into the strength and mode of binding of HM with DNA. The dynamical aspects of the interactions are also addressed through time-resolved emission and rotational relaxation dynamics studies. Our results indicate an intercalative mode of binding between the drug and the DNA, although the electrostatic interaction could not be ignored.

The enormous range of biological activities of the studied drug HM provided us the impetus to take the present study a step further, in which we endeavor to search for a simple strategy for dissociation of the drug from the drug−DNA complex. Deciphering of both the association and dissociation mechanisms of small drugs interacting with DNA is important to the field. Our results indicate that the simple technique of detergent-sequestered dissociation of the drug from drug−DNA complex can be a prospective strategy through a proper choice of detergent. In addition, the detergent-sequestration technique, that is, use of surfactant, provides some technical advantages, such as the cost-effectiveness of the method, easy to moderate reaction conditions to achieve the goal, and the surfactants being spectroscopically silent and relatively scatter-free, promote facile spectroscopic monitoring of the effects and so forth. Fluorescence kinetics measurements reveal a relatively slower rate of dissociation of the drug from the drug−DNA complex in the presence of the surfactant, in comparison with its binding with the DNA.

2. EXPERIMENTAL METHODS

2.1. Materials. Harmane (HM, Scheme 1) and herring sperm DNA procured from Sigma-Aldrich, USA were used as received. Tris buffer was purchased from SRL, India, and 0.01 M Tris−HCl buffer, pH 7.4, was prepared. Analytical grade urea from E-Merck was used after recrystallizing twice from MeOH (AR grade, Spectrochem, India). Potassium iodide (KI) and sodium chloride (NaCl) from E-Merck were used as supplied. The surfactants cetyltrimethyl ammonium bromide (CTAB), sodium dodecyl sulfate (SDS), and Triton X-100 (TX-100) were used as received from Sigma Chemical Co., U.S.A.

2.2. Instrumentations and Methods. *Steady-State and Time-Resolved Spectral Measurements.* The absorption and emission spectra were acquired on a Hitachi UV−vis U-3501 spectrophotometer and Perkin-Elmer LS55 fluorimeter, respectively. In all measurements, the concentration of the HM was maintained at 2.0 μM to avoid aggregation and reabsorption effects. Only freshly prepared solutions were used for spectroscopic measurements. Stock solutions of DNA were prepared by dissolving the solid material in buffer (pH = 7.4) and stored at 4 °C. The purity of the DNA sample was verified by monitoring the absorbance ratio at λ_{abs} = 260 nm to λ_{abs} = 280 nm (i.e., A_{260}/A_{280}), which was in the range 1.8−1.9.[6−9] The concentration of DNA was determined spectrophotometrically using the molar absorption coefficient ε_{DNA} = 12 858 cm^{-1} M^{-1} at λ_{abs} = 260 nm.[28] Spectral background corrections have been ensured by a similar set of solutions under experiment with the probe being omitted.

Scheme 1. Schematic of the Cation ⇌ Neutral Prototropic Equilibrium of HM[30]

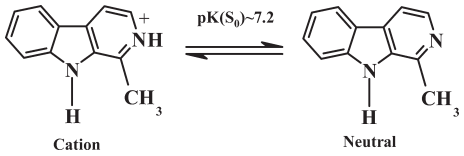

The fluorescence quantum yield (Φ_f) was calculated following the literature method[29] as described in the Supporting Information (section S1). Steady-state fluorescence anisotropy measurements were carried out on a Perkin-Elmer LS55 spectrofluorimeter (section S1 of the Supporting Information).

The fluorescence lifetime was determined from time-resolved fluorescence decay measured by the time-correlated single photon counting (TCSPC) technique.[29] The rotational relaxation dynamics (time-resolved fluoerescence anisotropy decay) was also monitored by the TCSPC technique. The details are given in the Supporting Information (section S1).

Circular Dichroism. Circular dichroism (CD) spectra were recorded on a JASCO J-815 spectropolarimeter using a cylindrical cuvette of 0.1 cm path length. The reported CD profiles are an average of four successive scans obtained at 20 nm/min scan rate with an appropriately corrected baseline. The concentration of DNA and the probe during CD measurements are mentioned in the relevant discussion.

Kinetics Measurement. The kinetics of association of HM with DNA and the kinetics of CTAB-induced dissociation of DNA-bound HM have been measured on a Perkin-Elmer LS55 spectrofluorimeter using the stopped-flow fluorescence measurement technique. The dead time of the instrument was found to be 20 ms.

All experiments were performed at an ambient temperature of 25 °C at pH = 7.4 unless otherwise specified. Only freshly prepared solutions were used for all measurements.

3. RESULTS AND DISCUSSIONS

3.1. Interaction of the Drug (HM) with DNA: The Strength and Mode of Binding. *3.1.1. Absorption Spectral Study.* HM in aqueous buffer medium exhibits two distinct broad absorption bands at $\lambda_{abs} \approx 348$ and ≈ 370 nm (Figure 1). The photophysical properties of various β-carboline derivatives have long been realized as an intriguing topic of research and have been addressed quite extensively in the literature.[30−37] In analogy to the literature reports,[30−37] the two absorption bands at ≈348 and ≈370 nm for HM (which is structurally similar and belongs to the same family of β-carbolines) in aqueous buffer are attributed to the neutral and cationic species of HM (Scheme 1), respectively.

It is documented that the relative intensities of the absorption bands of HM are sensitive to the surrounding environments, such as the nature of the solvent as well as extrinsically added additives.[30−37] Figure 1a reveals significant modification of the absorption profile of the drug HM upon interaction with DNA. Incremental addition of DNA to a solution of HM in aqueous buffer results in a progressive decrease in absorbance for the neutral species of HM at $\lambda_{abs} \approx 348$ nm with a concomitant increase in the cationic counterpart at $\lambda_{abs} \approx 370$ nm. Such changes of the absorption spectral properties of HM clearly

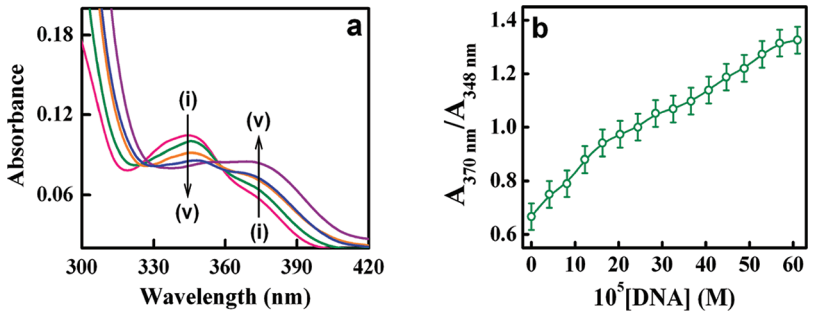

Figure 1. (a) Representative absorption profile of HM as a function of increasing concentration of DNA. Curves i−v correspond to 10^5[DNA] (M) = 0 (pink), 4.07 (green), 12.2 (orange), 20.33 (blue), and 44.72 (purple). (b) Variation of the absorbance of the cationic species of HM (λ_{abs} = 348 nm) relative to that of the neutral species (λ_{abs} = 370 nm) (i.e., $A_{370\ nm}/A_{348\ nm}$ ratio) as a function of DNA concentration.

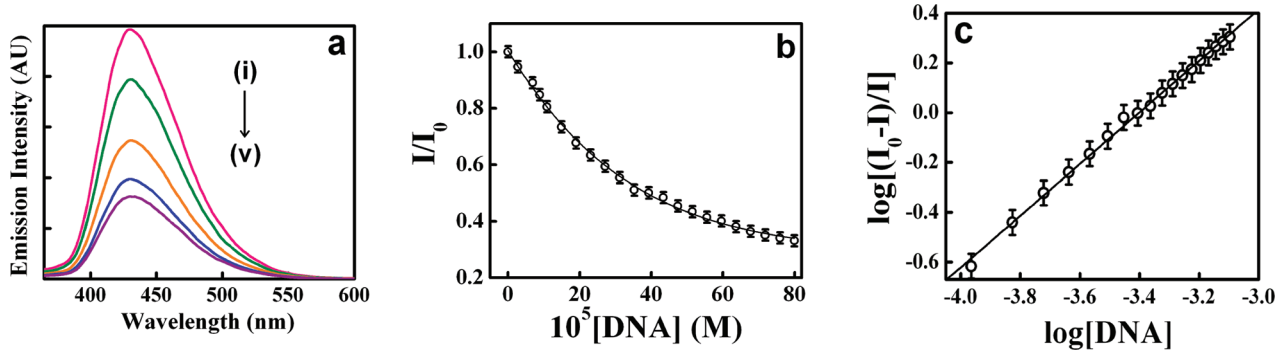

Figure 2. (a) Representative emission profile (λ_{ex} = 350 nm) of HM with increasing DNA concentration. Curves i−v correspond to 10^5[DNA] (M) = 0 (pink), 12.2 (green), 32.52 (orange), 60.98 (blue), 81.3 (purple). (b) Relative variation of cationic fluorescence of HM (I/I_0 at $\lambda_{em} \approx$ 435 nm; I_0 is the fluorescence intensity in the absence of DNA) as a function of DNA concentration. (c) Double logarithmic plot ($\log[(I_0 - I)/I]$ vs log[DNA]) for elucidation of the binding constant (K) for HM−DNA interaction from fluorescence data.

indicate that the prototropic equilibria of HM are enormously modified within the microheterogeneous DNA environment as compared with that in aqueous buffer.[35−37]

Figure 1b reflects that the ratio of $A_{cation}/A_{neutral}$ (i.e., $A_{370\ nm}/A_{348\ nm}$; A terms denote the absorbance values) is progressively enhanced as a function of DNA concentration. On the basis of this observation it can be argued that the ground state prototropic transformation of HM is remarkably favored to the cationic species in the presence of DNA. Favorable electrostatic stabilization between the cationic probe (HM) and negative polyphosphate DNA backbone may be invoked to interpret the observation. However, it is important to note in the present context that the DNA-induced absorption spectral changes of HM lack an isosbestic point (Figure 1a), indicating the operation of more than one type of interactions during the binding process. Hence, we have not employed the absorption study for the determination of the binding constant. This conjecture has been further substantiated from other experimental results to be discussed in forthcoming sections.

3.1.2. Emission Spectral Study. The DNA-induced modification to the steady-state emission spectral profile of the drug is depicted in Figure 2. The emission profile of HM in aqueous buffer medium is characterized by a single unstructured broad band at $\lambda_{em}^{max} \approx$ 435 nm, which is ascribed to the cationic species.[30−37] As displayed in Figure 2a, the cationic fluorescence of HM undergoes prominent quenching as a function of increasing DNA concentration with no appreciable shifting of the emission maximum. Figure 2b shows the relative variation (I/I_0) of cationic fluorescence of HM ($\lambda_{em} \approx$ 435 nm) against DNA concentration. The initial steep change in I/I_0 is found to be slowed down with increasing DNA concentration, probably marking the saturation of interaction between the drug and DNA.

Similar types of results were reported by Pal et al.[38] for modulation of photophysical properties of rhodamine derivatives in SDS micelle and also by Ghosh et al.[39] in their study of the interaction of 1-methylaminopyrene with anionic surfactants having different chain lengths.

Elucidation of Drug−DNA Binding Strength from Steady-State Emission Spectral Data. A quantitative rationalization of the drug−DNA binding strength is important in the evaluation of efficacy of the drug to function as a therapeutic agent. Here, we try to elucidate a quantitative assessment for the strength of the binding interaction between HM and DNA from the steady-state fluorescence quenching of HM with increasing DNA concentration (Figure 2). For this purpose, the quenching data have been treated in the following equation, which describes the equilibrium between free and bound molecules when small molecules bind independently to a set of equivalent sites in a macromolecule:[40]

$$\log\left[\frac{I_0 - I}{I}\right] = \log K + n \log[Q] \qquad (1)$$

in which K is the binding constant and n is the number of binding sites. Determination of binding parameters from fluorescence quenching data on the basis of the aforementioned equation (eq 1) has been extensively utilized in the literature.[40,41] Figure 2c reveals that the double logarithmic ($\log[(I_0 - I)/I]$ vs log[DNA]) plot for elucidation of HM-DNA binding strength

yields a linear regression with binding constant, K (±10%) = 3.34 × 10^3 M^{-1} and n = 1.03. This result, in comparison with literature reports,[6−10] indicates a moderately strong binding of the drug with DNA, and hence, natural inquisition strives one to search for a facile mode of dissociation of the DNA-bound drug. The facile dissociation of DNA-bound drug is, in fact, an important prerequisite for evaluation of the efficacy of the drug to function as a therapeutic agent, and this aspect has been explored in a forthcoming section.

Using the estimated value of the binding constant and the concentrations of HM and DNA, a maximum of ∼50% complex (for the highest DNA concentration) is calculated to be present in the sample. Therefore, it is necessary to evaluate whether the drug−DNA complex is fluorescent. Evaluation of the quenching data on the Stern−Volmer equation[29] has been processed to cast light on this issue. In addition, the associative binding constant for the drug−DNA complex as determined from the Stern−Volmer analysis is found to be in agreement with the value determined from the double logarithmic plot (vide Figure 2c, eq 1). The details are discussed in the Supporting Information (section S2).

3.1.3. Steady-State Fluorescence Anisotropy. A steady-state fluorescence anisotropy (r) study has been central in biochemical and biophysical research because of its ability to produce valuable information about the environments in the immediate vicinity of the fluorophore. The microenvironment of the probe molecule is governed by its precise location in the complex molecular assembly. Any modulation in the rigidity of the surrounding environment of the fluorophore gets reflected through anisotropy values. The so-called environment-induced motional restriction on the mobility of the probe in DNA[6,7,14−17,29,35−37] is manifested through anisotropy variation and thereby furnishes clues to assess the location of the probe within the complex biological environments. In the present case, the fluorescence anisotropy of HM (Figure 3) exhibits specific variation as a function of the DNA concentration. An initial steep rise in the anisotropy value implies the increasing degree of motional restriction on the probe molecules upon binding to DNA, which is then followed by a gradual saturation.

In fact, the variation of anisotropy of the fluorophore after binding to DNA is governed by more than one factor, such as (i) the three-dimensional shape and motions of DNA and the drug−DNA complex and (ii) the global Brownian tumbling of the drug−DNA complex.[6,7,14−17,29,35−37] Naturally, the overall dimension of the drug−DNA complex will be much larger compared with the unbound species per se and will, in turn, ensure a significant reduction in the overall tumbling motion of the former, leading to an increase in the anisotropy.[6,7,14−17,29,35−37]

The results of anisotropy measurement are used here to determine independently the drug−DNA binding constant. The binding constant determined from the steady-state anisotropy measurement (K = 9.4 × 10^3 M^{-1}) is found to be on the same order of magnitude compared with that obtained from emission intensity data (Section 3.1.2, vide Figure 2c). This observation not only establishes the reliability of the results, but also substantiates the practical applicability and feasibility of the methods employed for estimation of the binding constant. The methods are discussed in the Supporting Information (Section S3, Figure S2).

3.1.4. Effect of Ionic Strength. Since the drug HM carries positive charge and DNA has a negatively charged polyphosphate backbone the effect of ionic strength on HM-DNA binding interaction has been studied. The strong electrolyte NaCl has been employed to decipher the impact of electrostatic interaction between HM and DNA.[42,43] Increased ionic strength of the medium screens the electrostatic repulsion between consecutive phosphate groups (negatively charged), prompting the helix to shrink due to reduction in the unwinding tendency caused by the aforementioned electrostatic repulsion.[44] Thus, an increase in ionic strength of the medium will be associated with weakening of the electrostatic attraction between a positively charged fluorophore and DNA. Figure 4 reveals the effect of increasing ionic strength of the medium on the fluorescence properties of the DNA-bound probe. As seen in Figure 4a, increasing ionic strength of the medium results in fluorescence enhancement of the DNA-bound

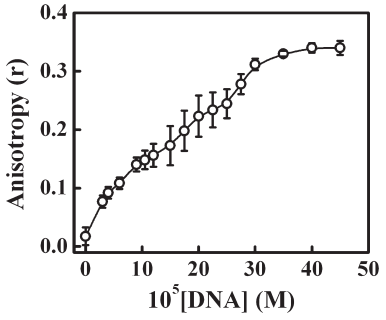

Figure 3. Variation of steady-state fluorescence anisotropy (r) of HM as a function of DNA concentration (λ_{ex} = 350 nm and $\lambda_{monitored}$ = λ_{em}^{max}). Each data point is an average of 15 individual measurements. Error bars are within the symbols if not apparent. The solid line represents only a visual guide to the pattern of variation.

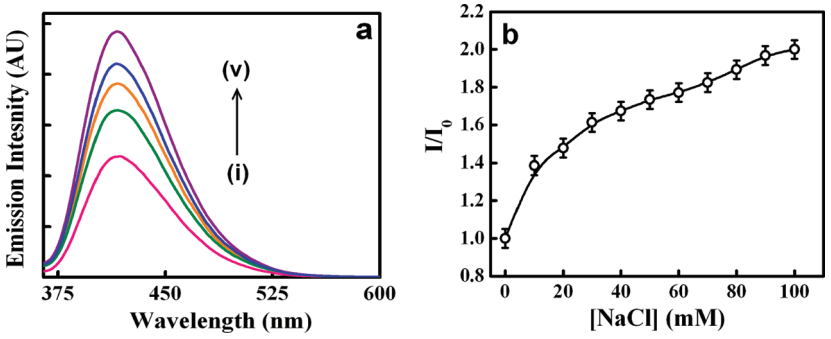

Figure 4. (a) Representative emission profile of DNA-bound HM with increasing ionic strength of the medium. Curves i−v correspond to [NaCl] (mM) = 0 (pink), 10 (green), 20 (orange), 50 (blue), 100 (purple). λ_{ex} = 350 nm and [DNA] = 54.2 × 10^{-5} M^{-1}. (b) Relative variation of cationic fluorescence (I/I_0 at $\lambda_{em} \approx$ 435 nm; I_0 is the fluorescence intensity in the absence of NaCl) of DNA-bound HM as a function of NaCl concentration. The solid line provides a visual guide to the pattern of variation.

dx.doi.org/10.1021/jp206589e |J. Phys. Chem. B 2011, 115, 11938–11949

probe. The variation of relative fluorescence intensity (I/I_0) at $\lambda_{em} \approx 435$ nm is shown in Figure 4b. This observation suggests that electrostatic interaction also plays a role in the HM−DNA interaction process. Involvement of more than one type of binding interaction (electrostatic interaction apart from intercalative binding) appears to justify the absence of an isosbestic point in the absorption study (Section 3.1.1, vide Figure 1a).

3.1.5. Steady-State Fluorescence Quenching. Monitoring the quenching of steady-state fluorescence of free HM (in aqueous buffer) and DNA-bound HM paves way for simple but efficient mapping of the mode of binding of the drug with DNA. When KI is employed as the quencher, the concept of the strategy lies in some simple modulations of the electrostatic interactions between the cationic probe (HM) and the anionic quencher (I^- ion). KI is found to be an effective quencher for the cationic drug HM ($\lambda_{em} \approx 435$ nm), as displayed in Figure 5, in which the quenching phenomenon has been followed on the Stern−Volmer equation:[14−17,29]

$$\frac{I_0}{I} = 1 + K_{SV}[Q] \qquad (2)$$

where I_0 is the original fluorescence intensity, I is the quenched intensity of the fluorophore (HM), [Q] is the molar concentration of the quencher (here, KI), and K_{SV} is the Stern−Volmer quenching constant. The higher the magnitude of K_{SV}, the more efficient the quenching, ensuring the greater is the degree of exposure of the quencher to the probe.[29] The results displayed in Figure 5 show a considerable reduction in quenching efficiency for the DNA-bound probe compared with the free (K_{SV} (±10%) = 436 M^{-1} for HM in aqueous buffer and 79.78 M^{-1} for HM in the presence of 90 × 10^{-5} M DNA. This concentration of DNA is chosen because it ensures the saturation of interaction between the probe and DNA (Section 3.1.2, vide Figure 2b)). This result supports an intercalative mode of binding of HM into the DNA double strands, since only the binding via intercalation should be able to screen the entrapped fluorophore from the ionic quencher, thereby ensuring a feeble interaction between the two (possible electrostatic repulsion between the negatively charged quencher and the negative polyphosphate backbone of DNA should also decrease interaction probability between the quencher and intercalated drug).[6,14−17,29,45,46] As for otherwise, electrostatic or groove binding should leave ample exposure of the fluorophore to the bulk aqueous buffer phase and is thus unlikely to resist a closer approach of the ionic quencher to the fluorophore.[6,9,14−17,29,45,46]

It is documented that the effective quenching efficiency of a quencher such as KI toward the fluorophore is reduced for intercalative binding but enhanced for groove binding, in comparison with that in aqueous buffer medium.[6,9,45−48] This is because KI by itself is a strong electrolyte that can release the fluorophore cations from the groove-bound condition on the DNA helix, thereby causing a decrease in the fluorescence yield, contrary to the protection of the fluorophore from the anionic quencher in the case of intercalation.[8,45−48] It is probably the contribution from electrostatic interaction in the drug−DNA binding process (Section 3.1.4) that KI-induced quenching efficiency of the DNA-bound drug is not negligible but, rather, quite fairly discernible (K_{SV} (± 10%) = 79.78 M^{-1}), even at a high concentration of DNA. This is not unlikely, since KI is also an electrolyte. Therefore, the effect of the ionic strength on the drug−DNA binding interaction, as discussed in Section 3.1.4, has been carried out with NaCl as the chloride ion has been found to be a poor quencher for the fluorescence of the drug.[50] This finding is also in agreement with a recent report.[50]

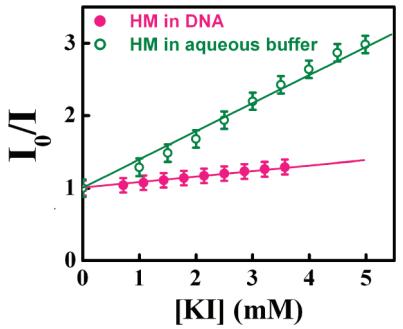

Figure 5. Stern−Volmer plot for I^- ion-induced quenching of steady-state fluorescence of HM in aqueous buffer and DNA environments. λ_{ex} = 350 nm and [DNA] = 90 × 10^{-5} M^{-1}. The respective environments are specified in the figure legend.

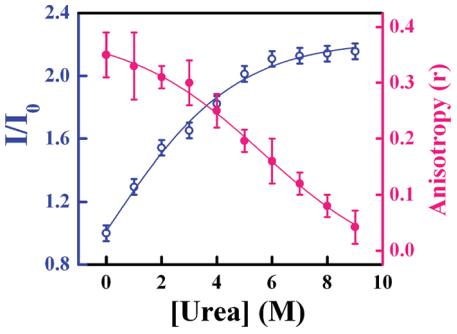

Figure 6. Variation of relative intensity of cationic fluorescence band of DNA-bound HM (I/I_0 at $\lambda_{em} \approx 435$ nm; I_0 is the fluorescence intensity in the absence of urea) and steady-state fluorescence anisotropy (each data point is an average of 15 individual measurements) of DNA-bound HM as a function of urea concentration. In each case, the solid line represents only a visual guide to the pattern of variation. λ_{ex} = 350 nm and [DNA] = 90 × 10^{-5} M^{-1}.

3.1.6. Chaotrope-Induced Perturbation of the Drug−DNA Binding Phenomenon. Here, the chaotrope-induced perturbation of the drug−DNA binding interaction has been attempted as complementary pathways to explore the binding phenomenon. Urea, which is a well-known denaturant for biopolymers, has been used as the chaotrope.[1,2,14−17,29,51−54] The effect of increasing the concentration of the chaotrope (urea) on the steady-state fluorescence properties of the DNA-bound drug (HM) is depicted in Figure 6 in the form of the relative variation of the cationic fluorescence of HM (I/I_0 at $\lambda_{em} \approx 435$ nm) as a function of chaotrope (urea) concentration, which is found to follow a qualitatively reverse pattern with respect to those reported in Figure 2b. The steady-state fluorescence anisotropy is also seen to be progressively decreased with increasing urea concentration (Figure 6), which suggests that the motional restriction on the probe imparted as a result of intercalation into the DNA helix is relaxed upon denaturation of the DNA.

That the presence of urea is found to induce changes to the photophysical properties of DNA-bound HM in a qualitatively reverse pattern with respect to those observed during the binding process is indicative of the fact that the probe preferentially binds to the B-form of DNA, and denaturation of DNA leads to considerable weakening of the binding.

In addition, it could be pertinent to note in the present context that the presence of urea is known to alter some solvent

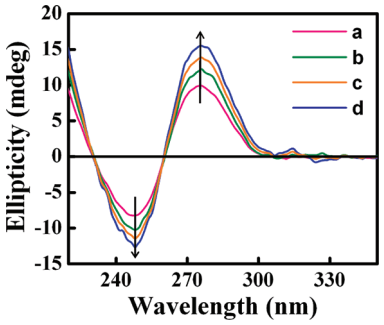

Figure 7. Circular dichroic spectral profile of DNA in the presence of varying concentrations of the drug. [HM] (μM) = 0 (a), 4.7 (b), 8.4 (c), 12.8 (d).

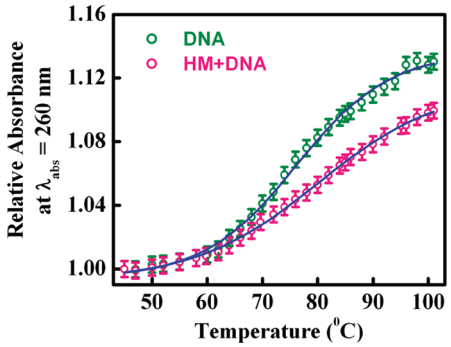

Figure 8. Thermal melting profiles of DNA and HM−DNA complex as constructed by observing the relative absorbance at λ_{abs} = 260 nm as a function of temperature.

properties, such as polarity, viscosity, refractive index, etc. Thus, it is worthwhile to consider the effect of increasing urea concentration on the monitored properties of the probe alone. For this purpose, the fluorescence spectra and steady-state fluorescence anisotropy of HM have been monitored in the presence of urea in a control experiment. Increasing the urea concentration (in the absence of DNA) is found to accompany only a slight increase in the fluorescence anisotropy (probably due to an increase in the viscosity of the solution in the presence of urea) and only insignificant perturbation of the emission intensity or λ_{em}^{max} position of HM. In short, urea-induced changes to the spectral properties of DNA-bound HM are found to be significantly larger in comparison with those in the absence of DNA. Therefore, it seems logical to consider that urea-induced denaturation of DNA plays the key role behind the present findings (Figure 6).

3.1.7. Circular Dichroic Spectral Study. The literature reflects an enormous application of the circular dichroic (CD) spectroscopic technique as a powerful tool in elucidating the modifications of the secondary structure of biopolymers as a result of interaction with small molecules.[1,2,6,14−17,29,50,55] Here, the perturbation in the secondary structure of DNA upon interaction with HM has been exploited by circular dichroism. Figure 7 shows the intrinsic CD spectrum of DNA in aqueous buffer at various concentrations of the extrinsically added probe. The intrinsic CD profile of DNA in the far-UV wavelength regime (220 − 320 nm) is characterized by a positive peak at ∼276 nm and a negative peak at ∼247 nm, which shows the signature of the right-handed B-form with 10.4 base pairs per turn, which is the normal form of DNA in aqueous buffer medium.[1−3,50,56−59] CD spectroscopy probes the asymmetry in a system, and the bands in the CD spectrum of B-DNA are said to emanate from the stacking interactions of the bases and the helical suprastructure of the polynucleotide, which provides asymmetric environments for the bases.[1,2,50,56−59]

Figure 7 reveals an enhancement in the CD signal of DNA with increasing concentration of HM. In analogy to the reported literature, the increase in the band intensity at ∼276 nm can be rationalized on the basis of disruption of the stacking contacts of the bases due to intercalation of the probe, which is required to optimize the binding interaction.[1,2,50,55−60] These changes thus reflect the modification in the relative orientation of the bases as required to accommodate the intercalated drug within a particular base pair.[1,2,50,56−61] On the other hand, it is reported that electrostatic or groove binding interactions can lead to only nominal perturbation of the intrinsic CD profile of DNA.[9,50,56−61] Thus, the result of circular dichroic analysis indicates an intercalative mode of binding of HM into the DNA helix.[1,2,6−9,50,56−61]

3.1.8. Helix Melting from Absorption Spectroscopy. The melting temperature (T_m) of DNA is defined as the temperature at which half of the DNA strands are in the double-helical state and half in the random-coil state.[9,62,63] The melting temperature depends on both the length and the specific nucleotide sequence of the molecule. Intercalation of small molecules into the DNA double helix is known to perturb the thermal stability of the latter, which will get manifested through modulation of the T_m. On the contrary, electrostatic or groove-binding interaction of small molecules with DNA leads to only insignificant modulation in T_m. This is readily understandable, since melting of the DNA helix requires rupture of the hydrogen bonding interactions between the base pairs, but electrostatic or groove-binding of a dye to DNA can hardly affect the same. It is only with the intercalative mode of binding of a dye that some perturbation in the hydrogen bonding interaction between the DNA base pairs and, hence, of the T_m can be expected. Therefore, any significant perturbation in the T_m of the DNA helix in the presence of the dye can lead a compelling evidence for the intercalative mode of binding.[8,9,62,63]

In the present study, we have monitored the change in T_m of the DNA upon interaction with HM to follow the mode of binding of HM with DNA. The DNA melting profile (in the absence and presence of the drug HM) has been constructed by monitoring the absorbance at 260 nm, which displays a hyperchromic shift with temperature.[9,62−65] Figure 8 clearly reflects the ability of HM to enhance the thermal stability of DNA (shifting of T_m ($\pm$1 °C) from ≈83 °C in the absence of HM to ≈87.5 °C in the presence of HM. The presently reported T_m for herring sperm DNA is in commendable conformity to the literature value[63−65]), which strongly supports the intercalative mode of binding of HM into the DNA helix.[9,62−65]

3.1.9. Modulation of Dynamics of HM upon Interaction with DNA. (a). Time-Resolved Fluorescence Decay. Fluorescence lifetime measurement often serves as a sensitive indicator of the local environment of a fluorophore and is responsive toward excited state interactions.[14−17,29−31,66−71] To delve into the photophysics of the drug within the DNA environment, the time-resolved fluorescence decay of HM has been recorded in the presence of DNA. In an attempt to follow a generalized picture of the interaction, we have chosen to record the fluorescence decays of HM in a series of varying concentrations of DNA. Some representative time-resolved decay profiles are displayed in Figure 9a, and the relevant data are summarized in Table 1. The drug

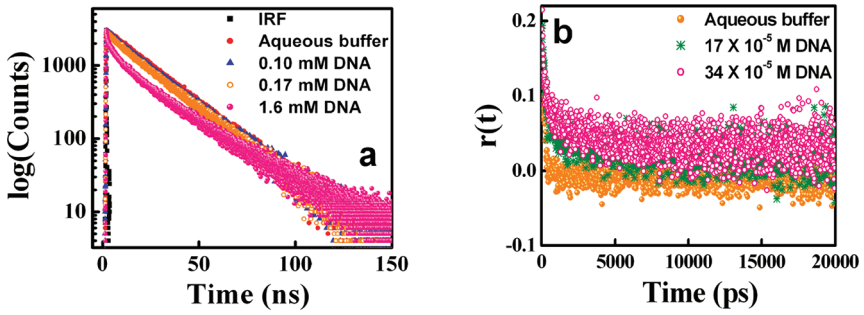

Figure 9. (a) Representative time-resolved fluorescence decay profile and (b) representative time-resolved fluorescence anisotropy decay profile of HM in aqueous buffer and DNA environments. Various concentrations of DNA are indicated in the respective legends. λ_{ex} = 340 nm $\lambda_{monitored} = \lambda_{em}^{max}$.

Table 1. Time-Resolved Fluorescence Decay Parameters of HM in Aqueous Buffer and DNA Environments

[DNA] (mM)	α_1[a] (%)	α_2[a] (%)	α_3[a] (%)	τ_1[a] (ns)	τ_2[a] (ns)	τ_3[a] (ns)	χ^2
0.0	100			21.67			1.09
0.10	63	6.1	31	21.13	5.78	0.14	1.01
0.17	59	10.05	31	21.57	6.14	0.22	1.07
0.56	55	14	31	22.01	6.51	0.30	1.18
0.64	37	26	37	24.36	7.27	0.50	1.2
1.13	40	30	31	26.02	7.74	0.63	1.27
1.6	42	29	29	26.58	7.72	0.68	1.27

[a] α_i is the pre-exponent corresponding to the ith decay time constant, τ_i. Standard deviation for the fitting analysis is ±8%.

Table 2. Different Photophysical Parameters of HM in Aqueous Buffer and DNA Environments

[DNA] (mM)	$\langle\tau_f\rangle$[a] (ns)	Φ_f[b]	k_r[c] × 10^{-7} (s^{-1})	k_{nr}[c] × 10^{-7} (s^{-1})
0.0	21.67	0.63	2.91	1.71
0.10	13.71	0.54	3.94	3.32
0.17	13.41	0.46	3.43	3.4
0.56	12.94	0.43	3.32	4.41
0.64	11.09	0.33	2.98	6.04
1.13	10.64	0.26	2.44	6.96
1.6	10.39	0.23	2.21	7.41

[a] $\langle\tau_f\rangle$ is the average fluorescence lifetime. [b] Φ_f (±2%) is the fluorescence quantum yield. [c] Radiative (k_r) and nonradiative (k_{nr}) decay rate constants.

molecule is found to exhibit a single-exponential decay pattern in the bulk aqueous buffer phase with a lifetime of τ = 21.67 ns.[30−34]

The data compiled in Table 1 reveal that in the DNA environment, the time-resolved fluorescence decay of the DNA-bound probe deviates significantly from a simple monoexponential pattern to a complicated triexponential function. Multiexponential decay of fluorescence in the microheterogeneous environment of DNA is not surprising,[6−9,14−17,29−31,66−71] but it is often difficult to assign specific mechanistic models to individual decay components; it could even be misleading in some cases.[14−17,29−31,66−71] (However, it is ethical to point out in the present context that from the binding constant K (±10%) = 3.34 × 10^3 M^{-1} (Section 3.1.2, Figure 2c) and using the concentrations of HM and DNA used, a maximum of ∼50% complex (for the highest DNA concentration) is calculated to be present in the sample. Thus, a possible contribution from the free (unbound) dye may be a probable factor for the observed multiexponential decay pattern (Table 1). Although the long decay component (τ_1 in Table 1) is close to the lifetime value of the probe in bulk aqueous buffer phase, a steady increase in the decay component, τ_1, is observed, along with a steady decrease in the relative amplitude, α_1, with increasing DNA concentration (Table 1). Hence, the situation may not be a simple case of multiexponential decay from differential populations of the fluorophore, in which assignment of specific mechanistic models to each decay component may be deceptive, at least within the present experimental window).

Therefore, it is rational to use the mean (average) fluorescence lifetime of HM for exploring its behavior within the DNA microheterogeneous environments, rather than emphasizing individual decay time constants.[14−17,29−31,66−71] The average lifetimes ($\langle\tau_f\rangle$) are presented in Table 2 (see also Section S1 of the Supporting Information). A glance at Table 2 reveals that the average lifetime of the drug progressively decreases with increasing DNA concentration and, thus, paves the way for assessing the degree of exposure of the probe to an aqueous buffer environment. A greater proximity between the lifetime values of the drug in aqueous buffer and DNA environments should reflect a greater degree of exposure of the drug to the aqueous environment. Thus, the data in Table 2 can be rationalized on the grounds of binding interaction between the probe and the DNA, resulting in the observed significant modifications in the fluorescence lifetime of HM.[14−17,29−31,66−71]

From the fluorescence yield (Φ_f) and average lifetime ($\langle\tau_f\rangle$) of HM in aqueous buffer and DNA environments, we have calculated the radiative (k_r) and nonradiative (k_{nr}) decay rate constants using the following two equations:[29]

$$k_r = \frac{\Phi_f}{\langle\tau_f\rangle} \quad (3)$$

$$k_{nr} = \frac{1}{\langle\tau_f\rangle} - k_r \quad (4)$$

The photophysical parameters collected in Table 2 unveil an enhancement of the k_{nr} with increasing DNA concentration. However, the modulation in the k_r is not so prominent. In fact, ideally, the k_r for HM should be a constant, since it represents a situation in which no other deactivation process is operative.[29] Thus, the observed alterations in the magnitude (Table 2) may be an outcome of the fact that the free (unbound) and bound drug populations are simultaneously present in the sample under

Table 3. Rotational Relaxation Dynamical Parameters from Time-Resolved Anisotropy Decay of HM in Aqueous Buffer and DNA Environments

10^5 [DNA] (M)	α_{1r} (%)	α_{2r} (%)	τ_{1r}[a] (ps)	τ_{2r}[a] (ns)	$\langle\tau_r\rangle$ (ns)	χ^2
0.0	100		124		0.124	1.2
17	91	9	317	9.34	1.13	1.05
25	82	18	325	10.97	2.24	1.05
34	76	24	335	12.59	3.28	1.08

[a] Standard deviation for the fitting analysis is ±5%.

investigation so that an average effect is observed within the experimental window[29]. Thus, the lowering of $\langle\tau_f\rangle$ of HM in the DNA environment can be attributed to the enhanced nonradiative rates. Further, these data reflect a strong corroboration to the observed modifications on the steady-state emission profile of HM (vide Figure 2, Section 3.1) in the sense that an increase in the k_{nr} for the cationic species of HM in the presence of DNA can be connected with lowering of emission intensity of the cationic species of HM (vide Figure 2a) as a function of DNA concentration.

(b). Rotational Relaxation Dynamics: Time-Resolved Fluorescence Anisotropy Decay. The time-dependent decay of fluorescence anisotropy is a sensitive indicator of the rotational motion or rotational relaxation of the fluorophore in an organized assembly.[14,29,66−71] Therefore, to explore the modulation of rotational relaxation dynamics of the drug within DNA environments, the time-resolved fluorescence anisotropy decay has been monitored in the absence and presence of DNA. Here also, our effort extends to follow the pattern of anisotropy decay as a function of increasing DNA concentration. The representative anisotropy decay profiles are given in Figure 9b, and the relevant rotational relaxation parameters are summarized in Table 3.

The fluorophore exhibits single exponential anisotropy decay (with a reorientation time of 124 ps) in aqueous buffer, whereas in the presence of DNA, the decay follows a biexponential pattern (with a slow and a fast reorientation time). The observation of a biexponential pattern in the anisotropy decay of HM in DNA with two different correlation times implies the presence of two dynamical processes occurring on different time scales.[29,66−71] The average rotational correlation time for HM in a paricular DNA concentration (Table 3) is found to be less than the average fluorescence lifetime in the same (Table 2), suggesting that the depolarization is essentially complete within the excited state lifetime of the probe in the specified environment.

The functional form of the biexponential anisotropy decay, $r(t)$, can be represented as[29]

$$r(t) = r_0 \times \left[\alpha_{1r} \exp(-t/\tau_{1r}) + \alpha_{2r} \exp(-t/\tau_{2r})\right] \quad (5)$$

in which r_0 is the limiting anisotropy that describes the inherent depolarization of the fluorophore and α_{ir} is the preexponent that provides the fraction of the ith rotational relaxation time, that is, τ_{ir}. Here, the generalized order parameter (S) is defined as $S^2 = \alpha_{2r}$. S describes the degree of restriction on the wobbling in cone orientational motion having values ranging from 0 (corresponding to unrestricted motion) to 1 (for complete restriction on the motion).

Note that in the present context, the limiting anisotropy value obtained from the time-resolved experiment (around 0.22) is found to be somewhat lower than the r_0 value obtained from steady-state anisotropy measurement (0.30 ± 0.01) in a medium of high viscosity (a mixture of glycerol/water = 90:10 by volume percentage). This probably reflects some rapid depolarization of the fluorescence.[14,29,67] On the other hand, it is a little puzzling to note that the steady-state anisotropy value in a 90:10 glycerol/water mixture is lower than that observed in the DNA environment at the saturation level of interaction (Section 3.1.3, vide Figure 3). It is, indeed, quite unusual to rationalize that the viscosity in the DNA is high enough to exceed the viscosity of a 90:10 glycerol/water mixture.[72] This observation probably implies the predominant role of some specific interactions (as can be rationalized in connection with an intercalative mode of binding, along with some contribution from electrostatic interaction) rather than the normal viscosity effect in governing the impartation of motional restrictions on the drug microenvironment upon interaction with the DNA.[73]

The data summarized in Table 3 are found to reflect a slowing down of the average rotational correlation time ($\langle\tau_r\rangle$) of HM with increasing DNA concentration as compared with that in an aqueous buffer phase. This suggests that the probe molecule experiences a motionally restricted environment in DNA.[29,66−71] The average rotational relaxation time has been calculated using the following equation:[29,67,69]

$$\langle\tau_r\rangle = \alpha_{1r}\tau_{1r} + \alpha_{2r}\tau_{2r} \quad (6)$$

Time-resolved anisotropy can be employed as a faithful tool to cast light on the distribution and location of the probe in the microheterogeneous environment. In principle, several arguments might emanate to account for the observed biexponential anisotropy decay behavior of the probe in DNA. First, the short (τ_{1r}) and the long (τ_{2r}) components of anisotropy decay can be argued to be coming from the rotational diffusion of the free (unbound) dye (HM) and the DNA-bound dye, respectively. However, for this proposition to be correct, the ratio α_{2r}/α_{1r} would give the ratio of DNA-bound dye to the free.[29,66−68] To verify the validity of this consideration, we have calculated the ratio of concentration of HM in DNA to that in an aqueous buffer phase following the method described in the literature (by Fayer et al., ref 68), and the value is found to be enormously smaller than the ratio α_{2r}/α_{1r}.[68] This result explicitly dictates that the observed anisotropy decay in the presence of DNA can be assigned on only the dynamics of the DNA-bound probe while negating any considerable contribution from the free (unbound) dye.[29,66−71]

Another possible interpretation for the biexponential anisotropy decay can be realized in connection with rotational diffusion of the probe bound to two distinct regions of DNA.[66,68] For this proposition to be correct, the coefficients α_{1r} and α_{2r} should reflect the relative probabilities of finding the dye in the two sites. From the data compiled in Table 3, it is evident that the probability of finding the probe in one interaction site is significantly larger than in the other ($\alpha_{1r} > \alpha_{2r}$).[29,66−68]

The aforementioned possibilities are hence invalidated, and the results appear to be in agreement with numerous studies in the literature.[29,66−71] The observed biexponential decay can thus be rationalized in terms of the probe undergoing different kinds of rotational motions in DNA.[29,66−71] This sort of an observation is often interpreted in light of the well-known *two-step and wobbling-in-cone* model,[66] according to which the fluorescence depolarization can be the result of three independent motions: (a) wobbling of the probe ($r_w(t)$) with a time constant τ_w, (b)

Table 4. Different Rotational Parameters for HM in the Presence of DNA as Calculated on the Basis of the Two-Step and Wobbling-in-Cone Model

10^5 [DNA] (M)	τ_w (ps)	S	θ_w (deg)	$D_w \times 10^{-8}$ (s^{-1})
17	328	0.30	65.04	7.06
25	335	0.42	57.04	6.06
34	344	0.49	52.48	5.27

translational motion of the probe ($r_D(t)$) along the surface of DNA with time constant τ_D, and (c) overall rotation of the DNA ($r_P(t)$) with a time constant τ_P.[29,66−71] The involvement of several kinds of motion leads to deviation of the decay of rotational function, $r(t)$, from a single exponential pattern. According to this model, the faster rotational relaxation (τ_{1r}) is described as the motion of a restricted rotor (probe) having its transition dipole moment undergoing orientational diffusion within a semicone of angle θ_w about an imaginary axis. Thus, the faster and slower rotational time constants can be written as[29,66−71]

$$1/\tau_w = 1/\tau_{1r} - 1/\tau_{2r} \quad (7)$$

The calculated values for the decay time constant associated with the wobbling motion of the probe (τ_w) are listed in Table 4.

Again, the semicone angle θ_w is related to the order parameter (S) through the following expression:[29,66−71]

$$S = \frac{1}{2}\cos\theta_w(1 + \cos\theta_w) \quad (8)$$

The increasing magnitude of the order parameter with increasing DNA concentration (Table 4) is consistent with the idea of an increasing degree of motional restriction imposed on the probe. This is further manifested in the decreasing value of the semicone angle, θ_w, with increasing DNA concentration; that is, the treatment of the so-obtained rotational dynamical parameters under the provision of the two-step and wobbling-in-cone model is found to successfully indicate an increasing degree of motional restriction imposed upon the probe molecule in the presence of DNA with respect to the bulk aqueous phase.

The wobbling diffusion coefficient (D_w) for the probe in DNA is obtained from the following equation:[29,66−71]

$$D_w = \frac{7{\theta_w}^2}{24\tau_w} \quad \text{for} \quad \theta_w \leq 30° \quad (9)$$

whereas for $\theta_w \geq 30°$, D_w is given as

$$D_w = \{(1-s^2)\tau_w\}^{-1}\left[\frac{x^2(1+x)^2}{2(x-1)}\left\{\ln\left(\frac{1+x}{2}\right) + \left(\frac{1-x}{2}\right)\right\} + \left(\frac{1-x}{24}\right)(6 + 8x - x^2 - 12x^3 - 7x^4)\right] \quad (10)$$

where $x = \cos\theta_w$.

Since in the present case θ_w is found to be >30° (Table 4), we have applied eq 10 in calculating the values of the wobbling diffusion coefficient (D_w), and the calculated values are collected in Table 4.

3.2. Surfactant-Induced Dissociation of the Drug−DNA Complex. The aforementioned discussions establish the strength and mode of binding interaction of the drug HM with the DNA.

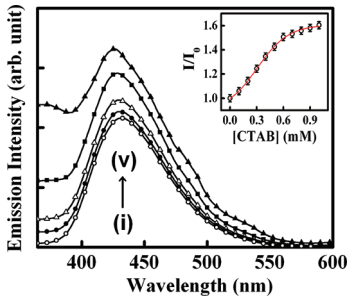

Figure 10. Effect of cationic surfactant CTAB on the emission profile (λ_{ex} = 350 nm) of DNA-bound HM. Curves i−v correspond to [CTAB] (mM) = 0 (○), 0.1 (●), 0.2 (Δ), 0.3 (■), 0.4 (▲). The inset shows the relative variation of cationic fluorescence (I/I_0 at $\lambda_{em} \approx 435$ nm; I_0 is the fluorescence intensity in the absence of CTAB) of DNA-bound HM with increasing CTAB concentration.

In this section, we endeavor to delve into the second aspect of the program, that is, dissociation of the drug from the drug−DNA complex.

The detergent-sequestration technique for dissociation of cationic drugs from DNA was first coined by Muller and Crothers in 1968[74] and has since elicited much attention.[74−78] In the present study, we attempt to establish that the conventionally accepted simple technique of using detergent molecules as the hydrophobic sink for dissociated drugs can be effectively applied for dissociation of HM from the HM−DNA complex by a proper choice of the detergent. Figure 10 depicts the changes in the emission profile of the DNA-bound HM with increasing concentration of a cationic surfactant cetyltrimethyl ammonium bromide (CTAB). The figure shows that surfactant CTAB-induced modifications to the emission profile of the DNA-bound HM occur qualitatively in a reverse pattern compared with those observed during the binding process (vide Section 3.1) along with the development of an additional band at $\lambda_{em} \approx 375$ nm. In direct analogy to literature reports, the new band at $\lambda_{em} \approx 375$ nm is ascribed to the neutral species of HM (Scheme 1).[30−37] The inset of Figure 10 shows that the relative variation (I/I_0) of the cationic fluorescence intensity of HM ($\lambda_{em} \approx 435$ nm) as a function of CTAB concentration follows a reverse trend with respect to that observed during binding of the HM with DNA (vide Figure 2b). This finding may be rationalized on the basis of surfactant-induced dissociation of the drug from the drug−DNA complex.

The spectral changes of the HM in the presence of CTAB alone are also monitored, and the details are mentioned in the Supporting Information (Section S4, Figure S3).

In this context, a direct comparison of the observations reported in Figure 10 with those in Figure S3 reveals a critical aspect of the present interaction scenario. Figure 10 reveals that CTAB imparts enhancement of emission intensity on both the neutral and the cationic counterparts of HM in the presence of DNA, and the effect of CTAB alone is different (enhancement of neutral emission with concomitant reduction of cationic emission, vide Figure S3 of the Supporting Information). Furthermore, CTAB-induced modulation of the emission profile of DNA-bound HM starts showing the onset for the saturation of interaction at a reasonably low CTAB concentration of ≈0.6 mM (Figure 10 inset), whereas CTAB alone can exert only insignificant perturbation to the emission profile of the drug up to such a low surfactant concentration.

Beyond [CTAB] ≈ 0.9 mM, the effect of a further increase in the CTAB concentration on the emission profile of DNA-bound

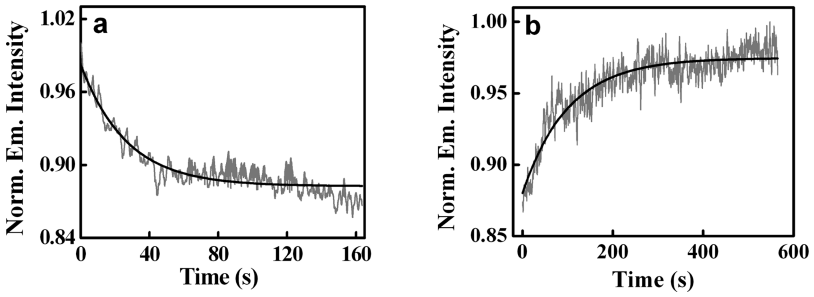

Figure 11. Change of fluorescence intensity (λ_{ex} = 350 nm, λ_{em} = 435 nm) of HM with time. (a) During interaction of HM (2.0 μM) with DNA (10×10^{-5} M). (b) Dissociation of DNA-bound HM in the presence of CTAB (0.9 mM). The solid black lines indicate the fitted lines.

HM is found to be analogous to those obtained in the absence of DNA. Therefore, it is logical to assign that CTAB-induced modulation in the emission profile of the DNA-bound drug as presented in Figure 10 is due to release of the intercalated drug from the DNA helix, resulting in enhancement of the cationic emission of HM, while at the same time the development of the neutral emission band of HM ($\lambda_{em} \approx 375$ nm) may be due to the increased hydrophobicity of the medium. The present results thus also indicate that only a low concentration of CTAB can be effective in inducing surfactant-sequestered dissociation of the cationic DNA-intercalated drug.

Similar effects were not observed with an anionic surfactant sodium dodecyl sulfate (SDS). This may be due to a lack of substantial interaction of SDS with DNA originating from an electrostatic repulsion from the negatively charged DNA polyphosphate backbone so that a close approach between DNA and SDS is energetically forbidden.[8,74−81] The neutral surfactant Triton X-100 was also tested for the present purpose, but the results could not be significantly improved in comparison with those observed with CTAB. This probably indicates the role of the electrostatic attraction between the cationic surface charge of the surfactant and the negative polyphosphate backbone of DNA, resulting in a closer approach between the two and, hence, favoring the interactions.

Surfactant molecules are known to form a micelle above a critical concentration (to be more specific, a narrow concentration range) called the critical micellar concentration (CMC). The CMC of CTAB in a pure aqueous environment is ~0.8 mM,[82] whereas in Tris−HCl buffer medium, the CMC is found to be lowered to about 0.17−0.20 mM.[82] From the inset of Figure 10, it is seen that the phenomenon of CTAB-induced dissociation of the DNA-bound drug starts showing the steep change at [CTAB] ≈ 0.2 mM and the onset of saturation of the interaction at [CTAB] ≈ 0.6 mM. It is thus logical to assume in the present context that in Tris−HCl buffer medium, the micellar structure is the active entity in inducing the observed surfactant (CTAB)-induced dissociation of the DNA-bound drug. This is not unlikely, since in this technique, the micelles are supposed to drive the equilibrium from the DNA-bound drug toward the dissociated drug by dumping the concentration of the free drug by absorption into the micelles.[75] The operation of this kind of a mechanism will obviously be effective with micellar structure rather than scattered surfactant molecules in the medium.[75−81]

It is pertinent to specify in this context that within the lower concentration region of CTAB, the presence of it does not perturb the native B-form of DNA, as has been evidenced from the CD spectrum of DNA in the presence of 0.6 mM CTAB, which resembles that of physiologically relevant B-DNA (figure not given).

3.3. Fluorescence Kinetics Study. In the study of the interaction of small drug molecules with DNA, both the association and dissociation kinetics are considered to have vital diagnostic importance.[74−78] The criterion of a slow rate of dissociation from DNA has been recognized as one of the most important properties for a drug to function as an efficient therapeutic agent.[74,75] The kinetics of the HM-DNA association reaction is studied by monitoring the quenching of HM fluorescence at λ_{em} = 435 nm upon interaction with DNA. A representative kinetic profile is displayed in Figure 11a, which leads to an observed association rate constant of k_a (±5%) = 0.0375 s^{-1}. Here, the observed fluorescence kinetic trace is fitted to a monoexponential decay function according to a pseudo-first-order reaction kinetics model, since the concentration of the DNA was significantly larger than that of the drug under the experimental conditions.[75] On the other hand, the cationic surfactant-induced dissociation kinetics monitored by fluorescence enhancement[83] of the DNA-bound drug at λ_{em} = 435 nm in the presence of CTAB (Figure 11b) is found to be much slower, as characterized by k_d (±5%) = 0.0098 s^{-1}. However, with a view to the fact that the dissociation kinetic rate constant determined in the presence of the surfactant (CTAB) cannot be directly compared with the dissociation rate constant in the absence of CTAB, we have used the following expression to estimate a value of the dissociation rate constant:

$$K = \frac{k_1}{k_{-1}} \tag{11}$$

in which the equilibrium constant is taken to be $K = 3.34 \times 10^3$ M^{-1} (Section 3.1.2), and k_1 and k_{-1} indicate the association and dissociation rate constants, respectively. The dissociation rate constant determined from eq 11 thus comes out to be $k_{-1} = 1.12 \times 10^{-5}$ M^{-1} s^{-1}.

Thus, the data imply that with the studied drug molecule, HM, the prerequisite of a relatively faster association kinetics with DNA and slower dissociation kinetics from DNA can be achieved. However, to obtain further details on the mechanism of the association/dissociation kinetics, more explicit experiments, including dependence of the rate constants on relevant extrinsic/intrinsic factors are required. In the present context, we refrain from making more elaborate comments on the issue, given the aim of the present work. Experiments along this direction are underway in our laboratory.

4. SUMMARY AND CONCLUSIONS

The present study reports the spectral deciphering of the binding interaction of a potent cationic biological photosensitizer, HM, with DNA. The photophysics and dynamics of the drug

molecule are found to be remarkably modified as a result of interaction with DNA in comparison with those in an aqueous buffer phase. From the series of studies undertaken in the present work, the mode of binding interaction of HM with DNA has been evidenced to be principally intercalative, although the electrostatic interaction between the cationic dye and DNA has also been argued. Concurrently, a chemical denaturation study reveals that the drug preferentially binds to the physiologically relevant B-form of DNA. Again, the cationic surfactant CTAB-induced modification to emission spectral characteristics of the DNA-bound drug reveals that the simple concept of detergent sequestration can be a prospective strategy for dissociation of the drug from the drug–DNA complex.

Overall, with a view to enormous biological applications and the promising prospects of β-carboline drugs on the field, the characterization of the strength, mode, and dynamics of binding of the drug with DNA is of potential importance and, hence, forms a demanding avenue of research. In the present report, we endeavor to unveil the scenario of β-carboline drug–DNA interaction with a potent member of the family, harmane (HM). We are optimistic that the presently exploited methodologies can be safely extended to other congeners, as well. Our results also throw light on the prospective probability of using HM as an efficient DNA probe.

■ ASSOCIATED CONTENT

Supporting Information. Information on the experimental methods, modified Stern–Volmer plot, binding constant from steady-state fluorescence anisotropy. and CTAB-induced modulation of emission spectra of HM. This information is available free of charge via the Internet at http://pubs.acs.org.

■ AUTHOR INFORMATION

Corresponding Author

*Phone: 91-33-2350-8386. Fax: +91-33-2351-9755. E-mail: nguchhait@yahoo.com.

■ ACKNOWLEDGMENT

B.K.P. thankfully acknowledges CSIR, India for a research fellowship. N.G. acknowledges DST, India for financial assistance through Project No. SR/S1/PC/26/2008. The authors greatly appreciate the cooperation received from Prof. Soumen Basak and Mr. Manas K. Sarangi of SINP, India for allowing us to use their TCSPC instrument. We are also grateful to the instrumental facilities of IACS, India for time-resolved anisotropy and CD measurements. The authors gratefully acknowledge the anonymous reviewers for their meticulous inspection of the work and constructive suggestions.

■ REFERENCES

(1) Berg, J. M.; Tymoczko, J. L.; Stryer, L. In *Biochemistry*, 5th ed.; Devlin, T. M., Ed.; W. H. Freeman and Company: New York, 2002.

(2) Lambert, B.; LePecq, J. B. In *DNA-Ligand Interactions, from Drugs to Proteins*; Guschlbauer, W., Saenger, W., Eds.; Plenum: New York, 1986.

(3) Acher, R. *Proteins and Nucleic Acids, Comprehensive Biochemistry*; Elsevier Publishing Company: New York, 1963; Vol. 8.

(4) Dervan, P. B. *Bioorg. Med. Chem.* **2001**, *9*, 2215–2235.

(5) Wahl, M; Koberling, F.; Patting, M.; Rahn, E. H. *Curr. Pharm. Biotechnol.* **2004**, *5*, 299–308.

(6) Gniazdowski, M.; Cera, C. *Chem. Rev.* **1996**, *96*, 619–634.

(7) Zhou, L.; Yang, J.; Estavillo, C.; Stuart, J. D.; Schenkman, J. B.; Rusling, J. F. *J. Am. Chem. Soc.* **2003**, *125*, 1431–1436.

(8) Cgen, Q.-y.; Li, D.-h.; Zhao, Y.; Yang, H.-h.; Zhu, Q.-z.; Xu, J.-g. *Analyst* **1999**, *124*, 901–906.

(9) Saha, I.; Hossain, M.; Kumar, G. S. *J. Phys. Chem. B* **2010**, *114*, 15278–15287.

(10) Rajski, S. C.; Williams, R. M. *Chem. Rev.* **1998**, *98*, 2723–2795.

(11) Rao, K. E.; Lown, J. W. *Chem. Res. Toxicol.* **1991**, *4*, 466–473.

(12) Langer, R. *Science* **2001**, *293*, 58–59.

(13) Barton, J. K. *J. Biomol. Struct. Dyn.* **1983**, *1*, 621–632.

(14) Paul, B. K.; Guchhait, N. *J. Phys. Chem. B* **2010**, *114*, 12528–12540.

(15) Paul, B. K.; Samanta, A.; Guchhait, N. *J. Phys. Chem. B* **2010**, *114*, 6183–6196.

(16) Paul, B. K.; Samanta, A.; Guchhait, N. *Langmuir* **2010**, *26*, 3214–3224.

(17) Hu, Y.-J.; Ou-Yang, Y.; Dai, C.-M.; Liu, Y.; Xiao, X.-H. *Biomacromolecules* **2010**, *11*, 106–112.

(18) Dey, D.; Pramanik, N. R.; Basu, S. *J. Phys. Chem. B* **2009**, *113*, 8689–8694.

(19) Bose, A.; Basu, S. *J. Phys. Chem. A* **2008**, *112*, 12045–12053.

(20) Choudhury, S. D.; Basu, S. *Spectrochim. Acta A* **2005**, *62*, 736–739.

(21) Bloom, F.; Barchas., J.; Sandler, M.; Usdin, E. *Progress in Clinical and Biological Research., Beta-carbolines and Tetrahydroisoquinolines*; Alan R. Liss Inc.: New York, 1982; Vol. 90.

(22) Braestrup, C.; Nielsen, M.; Olsen, C. E. *Proc. Natl. Acad. Sci. U. S.A.* **1980**, *77*, 2288–2292.

(23) Carlini, E. A. *Pharmacol., Biochem. Behav.* **2003**, *75*, 501–512.

(24) Dolmans, D. E. J. G. J.; Fukumura, D.; Jain, R. K. *Nat. Rev. Cancer* **2003**, *3*, 380–387.

(25) Allison, R. R.; Downie, G. H.; Cuenca, R.; Hu, X.-H.; Childs, C. J. H.; Sibata, C. H. *Photodiagn. Photodyn. Ther.* **2004**, *1*, 27–42.

(26) Henderson, B., Dougherty, T., Eds.; *Photodynamic Therapy: Basic Principles and Clinical Applications*; Marcel Dekker Inc.: New York, 1992.

(27) Chae, K. H.; Ham, H. S. *Bull. Korean Chem. Soc.* **1987**, *7*, 478–479.

(28) Leng, F. F.; Waldemar, P.; Chaires, J. B. *Biochemistry* **1998**, *37*, 1743–1753.

(29) Lakowicz, J. R. *Principles of Fluorescence Spectroscopy*; Plenum: New York, 1999.

(30) Coronilla, A. S.; Carmona, C.; Munoz, M. A.; Balon, M. *J. Fluoresc.* **2009**, *19*, 1025–1035.

(31) Wolfbeis, O. S.; Furlinger, E.; Wintersteiger, R. *Montash. Chem.* **1982**, *113*, 509–517.

(32) Balon, M.; Munoz, M. A.; Guardado, P.; Hidalgo, J.; Carmona, C. *Trends Photochem. Photobiol.* **1994**, *3*, 117–138.

(33) Tuveson, R. W. In *Light-Activated Pesticides*; Heitz, J. R., Downum, K. R., Eds.; ACS Symposium Series No. 339; American Chemical Society: Washington, DC, 1987; pp 192–205.

(34) Braestrup, C.; Nielsen, M.; Olsen, C. E. *Proc. Natl. Acad. Sci. U. S.A.* **1980**, *77*, 2288–2292.

(35) Reyman, D.; Pardo, A.; Poyato, J. M. L. *J. Phys. Chem.* **1994**, *98*, 10408–10411.

(36) Hayashi, K.; Nagao, M.; Gugimara, T. *Nucleic Acid Res.* **1977**, *4*, 3679–3685.

(37) Gonzalez, M. M.; Arnbjerg, J.; Denofrio, M. P.; Erra-Balsells, R.; Ogilby, P. R.; Cabrarizo, F. M. *J. Phys. Chem. A* **2009**, *113*, 6648–6656.

(38) Pal, P.; Zeng, H.; Durocher, G.; Girard, D.; Giasson, R.; Blanchard, L.; Gaboury, L.; Illeneuve, L. *J. Photochem. Photobiol. A* **1996**, *98*, 65–72.

(39) Ghosh, S. K.; Pal, A.; Kundu, S.; Mandal, M.; Nath, S.; Pal, T. S. *Langmuir* **2004**, *20*, 5209–5213.

(40) Connors, K. A. *Binding Constants. The Measurements of Molecular Complex Stability*; Wiley: New York, 1987.

(41) Abou-Zied, O. K.; Al-Shihi, O. I. K. *J. Am. Chem. Soc.* **2008**, *130*, 10793–10801.

(42) Cao, Y.; He, X. W. *Spectrochim. Acta, Part A* **1998**, *54*, 883–892.
(43) Chuan, D.; Yu-xia, W.; Yan-li, W. *J. Photochem. Photobiol. A* **2005**, *174*, 15–22.
(44) Modukuru, N. K.; Snow, K. J.; Perrin, B. S.; Kumar, C. V. *J. Phys. Chem. B* **2005**, *109*, 11810–11818.
(45) Berman, H. M.; Young, P. R. *Annu. Rev. Biophys. Bioeng.* **1981**, *10*, 87–114.
(46) Lerman, L. S. *J. Mol. Biol.* **1961**, *3*, 18–30.
(47) Kumar, C. V.; Asuncion, E. H. *J. Chem. Soc.: Chem. Commun.* **1992**, *6*, 470–472.
(48) Kumar, C. V.; Turner, R. S.; Asuncion, E. H. *J. Photochem. Photobiol. A* **1993**, *74*, 231–238.
(49) Martin, L.; Olives, A. I.; del Castillo, B.; Martin, M. A. *Luminescense* **2005**, *20*, 152–161.
(50) Sarkar, D.; Das, P.; Basak, S.; Chattopadhyay, N. *J. Phys. Chem. B* **2008**, *112*, 9243–9249.
(51) Canchi, D. R.; Paschek, D.; Garcia, A. E. *J. Am. Chem. Soc.* **2010**, *132*, 2338–2344.
(52) Priyakumar, U. D.; Hyeon, C.; Thirumalai, D.; MacKerell, A. D., Jr. *J. Am. Chem. Soc.* **2009**, *131*, 17759–17761.
(53) Sagle, L. B.; Zhang, Y.; Litosh, V. A.; Chen, X.; Cho, Y.; Cremer, P. S. *J. Am. Chem. Soc.* **2009**, *131*, 9304–9310.
(54) Gabel, F.; Ringkjobing, M.; Zacca, G.; Blackledge, M. *J. Am. Chem. Soc.* **2009**, *131*, 8769–8771.
(55) Jain, S. S.; Matjaz, A.; Hud, N. V. *Nucleic Acids Res.* **2003**, *31*, 4608–4615.
(56) Bonincontro, A.; Falivene, M.; LaMesa, C.; Risuleo, G.; Ruiz Pena, M. *Langmuir* **2008**, *24*, 1973–1978.
(57) Long, Y. F.; Liao, Q. G.; Zhi Huang, C.; Ling, J.; Li, Y. F. *J. Phys. Chem. B* **2008**, *112*, 1783–1788.
(58) Van Holde, K.; Johnson, W. C.; Ho, P. S. *Principles of Physical Biochemistry*; Prentice Hall: New York, 1998.
(59) Garbett, N. C.; Ragazzon, P. A.; Chaires, J. B. *Nature Protocols* **2007**, *2*, 3166–3172.
(60) Monnot, M.; Mauffret, O.; Lescot, E.; Fermandjian, S. *Eur. J. Biochem.* **1992**, *204*, 1035–1039.
(61) Tietze, L. F.; Krewer, B.; Major, F.; Schuberth, I. *J. Am. Chem. Soc.* **2009**, *131*, 13031–13036.
(62) Santalucia, J. *Proc. Natl. Acad. Sci. U.S.A.* **1998**, *95*, 1460–1465.
(63) Mergny, J. L.; Duval-Valentin, G.; Nguyen, C. H.; Perrouault, L.; Faucon, B.; Rougee, M.; Montenay Garestier, T.; Bisagni, E.; Helene, C. *Science* **1992**, *256*, 1681–1684.
(64) Zhong, W.; Yu, J.-S.; Liang, Y. *Spectrochim. Acta* **2003**, *59*, 1281–1288.
(65) Patel, D. J. *Acc. Chem. Res.* **1979**, *12*, 118–125.
(66) Kinosita, K.; Kawato, S.; Ikegami, A. *Biophys. J.* **1977**, *20*, 289–305.
(67) Dutt, G. B. *J. Phys. Chem. B* **2005**, *109*, 4923–4928.
(68) Quitevis, E. L.; Marcus, A. H.; Fayer, M. D. *J. Chem. Phys.* **1993**, *97*, 5792–5769.
(69) Chakraborty, A.; Seth, D.; Setua, P.; Sarkar, N. *J. Chem. Phys.* **2008**, *128*, 204510–204519.
(70) McKenna, C. E.; Kashemirov, B. A.; Upton, T. G.; Batra, V. K.; Goodman, M. F.; Pedersen, L. C.; Beard, W. A.; Wilson, S. H. *J. Am. Chem. Soc.* **2007**, *129*, 15412–15413.
(71) Sahoo, D.; Bhattacharya, P.; Chakravorti, S. *J. Phys. Chem. B* **2010**, *114*, 2044–2050.
(72) Sakai, H.; Takeoka, S.; Wettstein, R.; Tsai, A. G.; Intaglietta, M.; Tsuchida, E. *Am. J. Physiol.: Heart Circ. Physiol.* **2002**, *283*, 1191–1199.
(73) Chakrabarty, A.; Mallick, A.; Haldar, B.; Das, P.; Chattopadhyay, N. *Biomacromolecules* **2007**, *8*, 920–927.
(74) Muller, W.; Crothers, D. M. *J. Mol. Biol.* **1968**, *35*, 251–290.
(75) Westerlund, F.; Wilhelmsson, L. M.; Norden, B.; Lincoln, P. *J. Am. Chem. Soc.* **2003**, *125*, 3773–3779.
(76) Gabbay, E. J.; Grier, D.; Fingerle, R. E.; Reimer, R.; Levy, R.; Pearce, S. W.; Wilson, W. D. *Biochemistry* **1976**, *15*, 2062–2070.
(77) Wilson, D. W.; Grier, D.; Reimer, R.; Bauman, J. D.; Preston, J. F.; Gabbay, E. J. *J. Med. Chem.* **1976**, *19*, 381–384.
(78) Fox, K. R.; Brassett, C.; Waring, M. J. *Biochim. Biophys. Acta* **1985**, *840*, 383–392.
(79) Wakelin, L. P. G.; Atwell, G. J.; Rewcastle, G. W.; Denny, W. A. *J. Med. Chem.* **1987**, *30*, 855–861.
(80) White, R. J.; Phillips, D. R. *Biochem. Pharmacol.* **1988**, *38*, 331–334.
(81) Phillips, D. R.; Greif, P. C.; Boston, R. C. *Mol. Pharmacol.* **1988**, *33*, 225–230.
(82) Geng, F.; Yu, L.; Lu, T.; Li, Z.; Zheng, L.; Li, G. *J. Dispersion Sci. Technol.* **2008**, *29*, 1209–1213.
(83) Kaya, A. I.; Thaker, T. M.; Preininger, A. M.; Iverson, T. M.; Hamm, H. E. *Biochemistry* **2011**, *50*, 3193–6203.